Vol. 02, Iss. 4 (2025) 163-185, DOI: 10.61552/JSI.2025.04.001

Journal of Sustainable Development Innovations

www.jsi.aspur.rs

Static Behavior of Anti-symmetric Angle-ply Composite Stiffened Cylindrical Shell with Cutout

Sudip Kr Halder[a], Anirban Mitra[a], Sarmila Sahoo[b,*]

[a]*Department of Mechanical Engineering, Jadavpur University, Kolkata 700032, India,*
[b]*Department of Civil Engineering, Heritage Institute of Technology, Kolkata 700107, India.*

Keywords:

Cylindrical shell; Anti-symmetric angle-ply; Stiffener; Cutout; Finite element method.

* Corresponding author:

Sarmila Sahoo
E-mail: sarmila.sahoo@gmail.com

Received: 17 November 2024
Revised: 18 December 2024
Accepted: 19 January 2025

A B S T R A C T

The present work examines the static behavior of a laminated anti-symmetric angle-ply stiffened cylindrical shell in presence of cutout. The first-order shear deformation theory is used to model the stiffeners as well as the shell panel. The stiffeners and the shell panel surface are modeled using three-noded beam elements and eight-noded curved quadratic isoparametric elements respectively. Fiber orientation angle, layer numbers and six distinct boundary conditions are considered as the variables for the current study. The dimensionless values of displacement under static condition and stress resultants are calculated. The relative performance analysis of each shell combination is ranked based on their displacement and stress resultants. Several additional issues related to anti-symmetric angle-ply laminated stiffened composite cylindrical shells are also addressed.

1. INTRODUCTION

Composite materials are extensively utilized in various applications such as marine, automotive, mechanical, civil and aerospace industries. It offers unique advantages such as high stiffness-to-weight ratio, high strength-to-weight ratio, and improved load-bearing capacity, better resistance to buckling, excellent vibration damping performance and lightweight properties. Lamination is done to composite materials to enhance their mechanical properties, such as strength and stiffness. It also improves durability and resistance to environmental factor. It enables the optimization of material performance by integrating layers with varying orientations and properties. Cylindrical shell panels made of laminated composite materials are widely used in the aforementioned applications because it can also offers efficient distribution of internal or external pressure loads. Sometimes cutouts are made in cylindrical shell structures for creating a passage for pipelines or electrical equipment or air vents. In some cases, cutouts are used for repairs and altering resonance frequencies. In many cases cutout is required to place the sensors in the

appropriate position to monitor the structural health and conditions. Thin cylindrical shell structures with cutouts typically exhibit enhanced performance when fitted with stiffeners. A stiffener increases the stability of the shell structure with cutouts. Fundamental understanding of the static behavior with respect to deflection, forces and moment resultants of composite stiffened cylindrical shell in presence of cutout under various boundary conditions is essential for applying these designs effectively.

A concise literature review relevant to the current study is presented here. A thorough scrutiny of available literature review identifies the gaps in knowledge, informs the development of novel methodologies and guides future research directions in this field. The study of stiffened cylindrical shell using finite element analysis has been started by Kohnke and Schnobrich [1]. Later studies of stiffened cylindrical shells under different conditions are being continued. The bending behavior of composite stiffened hypar shells under concentrated loads has been studied by Sahoo and Chakravorty [2]. The analysis of the effects of free-edge on anti-symmetric angle-ply laminated shell panels under uniform axial extension has been conducted by Miri and Nosier [3]. The static behavior and structural performance through FEA of stiffened hypar shells with cutouts have been investigated by Chowdhury et al. [4]. The bending behavior of composite laminated cylindrical shell panels with arbitrary end-support conditions has been evaluated by Kumari and Kar [5]. The steady-state responses in laminated composite cylindrical shells have been analyzed by Zhu et al. [6]. Various parametric studies have been carried out by varying the positions relative to the cylindrical shell center and adjusting cutout sizes under different edge conditions by Savine et al. [7]. The influence of process parameters on free vibration of truncated laminated symmetric and anti-symmetric cross-ply laminated orthotropic thin shells was studied by Najafov et al. [8]. Vibration analyses of laminated composite skew cylindrical shells have been investigated using higher order shear deformation theory by Kumar et al. [9]. The effects of various parameters on frequency of anti-symmetric angle-ply cylindrical shells by first-order shear deformation theory have been investigated by Viswanathan and Javed [10]. Three-dimensional vibration analysis of arbitrary angle-ply laminated cylindrical shells under different boundary conditions has been studied by Tong et al. [11]. The nonlinear vibration analyses of laminated composite angle-ply cylindrical and conical shells have been investigated by Mohammadrezazadeh and Jafari [12]. Nonlinear dynamic models through finite element simulation for anti-symmetric cross-ply laminated shells made of glass fiber resin have been developed by Zhang and Zhang [13]. Chaudhuri et al. [14] have examined the dynamic behavior of stiffened composite cylindrical shells with cutout. They pointed out the impact of laminate configuration and boundary constraints on vibration characteristics. The failure behaviors of laminated composite stiffened cylindrical panels have been performed by Keshav et al. [15]. The buckling behavior of composite stiffened cylindrical cutout shell panels using finite element analysis (FEA) has been investigated by Sahoo [16]. The buckling study in composite cylindrical shell panels under lateral loads have been performed by Liang and Li [17]. The multi-objective model for an anti-symmetric cylindrical shell has been optimized by Sun et al. [18]. A novel analysis method for lattice composite cylindrical shells reinforced with graphene platelets nano particles has been introduced by Dai and Kiani [19]. A review of research articles focusing on composite cylindrical shells has been conducted by Zhang et al. [20].

Cylindrical shells made of composite materials have received considerable attention from researchers. Dimensionless values of displacement under static condition and stress resultants are important aspects of bending studies. It is essential to restrict the downward deflection and stress resultants within acceptable limits to avoid failure due to natural disturbances. Upon conducting the literature review, it was found that there is existing research present on the bending behavior of stiffened composite hypar shell with cutout. But, it becomes apparent that there is no literature that considers the bending behavior of stiffened cylindrical shell with cutout made of anti-symmetric angle-ply laminated composites under various boundary conditions. Understanding the behavior of the said

structure under static loading is crucial for the efficient utilization. The primary objective of this investigation is to examine the aforementioned structure to enhance overall effectiveness. The present study focuses on comparative performance analysis of the said cylindrical structure. The mechanical properties and structural performance of the composite shell are directly influenced by many factors. But, it is not possible to consider the effect of all these parameters in a single study. Accordingly, the present study employs the factors that significantly affect the behavior. The fiber orientation angle, number of layers and six distinct boundary conditions are considered as variable parameters. These studies can lead to the accurate use of cylindrical shell structures.

2. MATHEMATICAL FORMULATION

A thin stiffened cylindrical shell with cutout of uniform thickness (h) made of composite is considered for the present study as shown in Figure 1. The surface equation of any shell form can be represented by the equation z = f (x, y). The shell curvature is expressed as $\frac{1}{R_y} = \frac{d^2z}{dy^2}$.

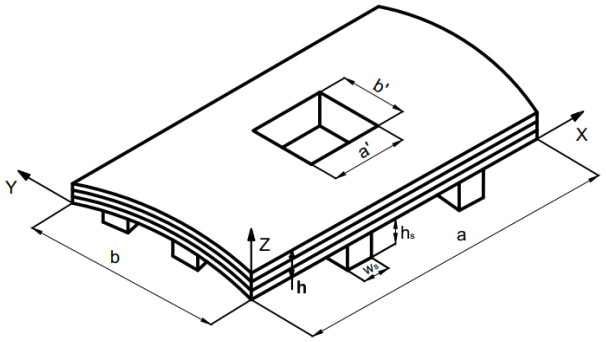

Fig. 1. Stiffened cylindrical shell with cutout.

The radius of curvature of the shell along global Cartesian coordinates Y direction is R_y. In Figure 1, a denotes length and b denotes width in the structure, $a^{/}, b^{/}$ represent the cutout length and width respectively.

The shell panel is modeled by an eight-node curved quadratic isoparametric finite element having four corner nodes and four mid-side nodes. This is depicted in Figure 2. The five degrees of freedom including three translations such as u, v, w and two rotational α, β are considered at each node.

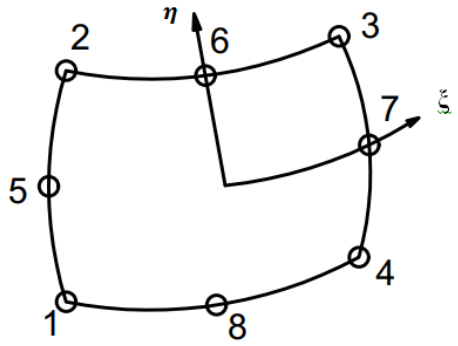

Fig. 2. Eight-noded isoparametric shell element.

The subsequent equations define the relationships between the coordinates ξ and η and the displacement at any specific point. The nodal degree of freedom is also addressed by these equations. The standard notations are utilized for the present analysis.

$$u = \sum_{i=1}^{8} N_i u_i, \quad v = \sum_{i=1}^{8} N_i v_i, \quad w = \sum_{i=1}^{8} N_i w_i$$
$$\alpha = \sum_{i=1}^{8} N_i \alpha_i, \beta = \sum_{i=1}^{8} N_i \beta_i \qquad (1)$$

The isoparametric formulation relies on the same shape function for its formulation i.e.

$$x = \sum_{i=1}^{8} N_i x_i, \qquad y = \sum_{i=1}^{8} N_i y_i \qquad (2)$$

A cubic interpolation polynomial is utilized for deriving the shape functions. The same can be expresses as follows:

$$N_i = \frac{(1+\xi\xi_i)(1+\eta\eta_i)(\xi\xi_i+\eta\eta_i-1)}{4}, \text{ for } i = 1, 2, 3, 4$$
$$N_i = \frac{(1+\xi\xi_i)(1-\eta^2)}{2}, \text{ for } i = 5, 7$$
$$N_i = \frac{(1+\eta\eta_i)(1-\xi^2)}{2}, \text{ for } i = 6, 8 \qquad (3)$$

Where, N_i denotes the shapes function at i-th node.

The generalized displacements at any point within the element can be interpolated from the nodal values as

$$[u] = [N]\{d_e\} \qquad (4)$$

Where,

$$\{u\} = \begin{Bmatrix} u \\ v \\ w \\ \alpha \\ \beta \end{Bmatrix} = \sum_{i=1}^{8} \begin{bmatrix} N_i & & & & \\ & N_i & & & \\ & & N_i & & \\ & & & N_i & \\ & & & & N_i \end{bmatrix} \begin{Bmatrix} u \\ v \\ w \\ \alpha \\ \beta \end{Bmatrix}$$

Generalized force and moment resultants in the cylindrical shell structure are displayed in Figure 3.

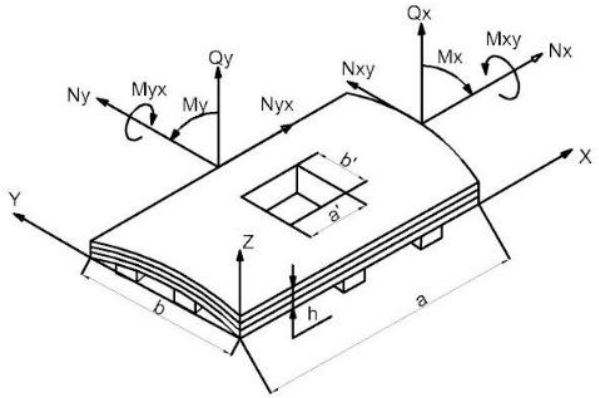

Fig. 3. Generalized force and moment resultants.

The constitutive equations for the shell are given by

$$\{F\} = [D]\{\varepsilon\} \tag{5}$$

The aforementioned equations can be computed by

$$\{F\} = \{N_x\ N_y\ N_{xy}\ M_x\ M_y\ M_{xy}\ Q_x\ Q_y\},$$
$$\{\varepsilon\} = \{\varepsilon_x^0\ \varepsilon_y^0\ \gamma_{xy}^0\ k_x\ k_y k_{xy}\ \gamma_{xz}^0 \gamma_{yz}^0\}^T$$

and [D] is the laminate stiffness matrix utilized in this study and are based on the work presented by Sahoo and Chakravorty [21].

The strain components for generalized representation of the three-dimensional strain field can be expressed in the form of

$$\{\varepsilon\} = [B]\{d_e\} \tag{6}$$

The above ε value can be calculated by

$$\{d_e\} = \{u_1\ v_1\ w_1\ \alpha_1\ \beta_1 \ldots\ u_8\ v_8\ w_8\ \alpha_8\ \beta_8\}^T$$

and

$$[B] = \sum_{i=1}^{8} \begin{bmatrix} N_{i,x} & 0 & 0 & 0 & 0 \\ 0 & N_{i,y} & 0 & 0 & 0 \\ N_{i,y} & N_{i,x} & -N_{i,y}/R_y & 0 & 0 \\ 0 & 0 & 0 & N_{i,x} & 0 \\ 0 & 0 & 0 & 0 & N_{i,y} \\ 0 & 0 & 0 & N_{i,y} & N_{i,x} \\ 0 & 0 & N_{i,x} & N_i & 0 \\ 0 & 0 & N_{i,y} & 0 & N_i \end{bmatrix}$$

According to the modified Sanders' first approximation theory for thin shells, the strain-displacement relationships are established as

$$\{\varepsilon_x, \varepsilon_y, \gamma_{xy}, \gamma_{xz}, \gamma_{yz}\}^T = \{\varepsilon_x^0, \varepsilon_y^0, \gamma_{xy}^0, \gamma_{xz}^0, \gamma_{yz}^0\}^T + z\{k_x, k_y, k_{xy}, k_{xz}, k_{yz}\}^T \tag{7}$$

Where, where the first vector on the right hand side represents the mid-surface strains and the second vector represents the curvatures of the shell.

The following element stiffness matrix is used for calculating K_{she} as:

$$[K_{she}] = \iint [B]^T [D][B] dxdy \tag{8}$$

The two-dimensional integral is transformed to isoparametric coordinates and is evaluated by two-point Gauss quadrature.

The FEA formulation for the stiffener is also performed. Stiffeners are oriented along X and Y-directions. Three noded curved isoparametric elements are taken along the cutout boundaries. The stiffener shape functions are expressed as follows:

For x-stiffeners:

$$N_{\xi i} = \xi\xi_i(1 + \xi\xi_i) \quad \text{for i=1, 3}$$
$$N_{\xi i} = (1 - \xi^2) \quad \text{for i =2} \tag{9}$$

For y-stiffeners:

$$N_{\eta i} = \eta\eta_i(1 + \eta\eta_i) \quad \text{for i=1, 3}$$
$$N_{\eta i} = (1 - \eta^2) \quad \text{for i =2} \tag{10}$$

Four degrees of freedom consisting two translation u, w and two rotational α, β at each node is considered for both x-stiffeners and y-stiffeners. The displacement field at any point

can be expressed in terms of nodal displacements as follows:

$$\text{For x-stiffeners: } \{\delta_{sx}\} = [N_{\varepsilon i}]\{\delta_{sxi}\}$$
$$\text{For y-stiffeners: } \{\delta_{sy}\} = [N_{\eta i}]\{\delta_{syi}\} \quad (11)$$

The generalized force-displacement for stiffeners is expressed as:

$$\{F_{sx}\} = [D_{sx}]\{\varepsilon_{sx}\} = [D_{sx}]\{B_{sx}\}\{\delta_{sxi}\}$$
$$\{F_{sy}\} = [D_{sy}]\{\varepsilon_{sy}\} = [D_{sy}]\{B_{sy}\}\{\delta_{syi}\} \quad (12)$$

The element stiffness matrixes for the stiffeners are expressed as:

$$[K_{xe}] = \int [B_{sx}]^T [D_{sx}][B_{sx}]dx \quad \text{for x-stiffener}$$
$$[K_{ye}] = \int [B_{sy}]^T [D_{sy}][B_{sy}]dy \quad \text{for y-stiffener} \quad (13)$$

2-point Gauss quadrature is used for evaluating the stiffness after converting the integrals to isoparametric coordinates.

Finally, the element stiffness matrix for the stiffened shell is achieved by connecting the nodes of shell elements with stiffeners using a connectivity matrix. This element stiffness matrix is then presented as:

$$[K_e] = [K_{she}] + [K_{xe}] + [K_{ye}] \quad (14)$$

The consistent load vector $\{P_e\}$ is given by

$$\{P_e\} = \iint [N^T]\{q\}\, dx\, dy \quad (15)$$

Where the scalar q is uniformly distributed transverse load. The area integral is evaluated by two-point Gauss quadrature like stiffness matrix.

2.1 Solution Procedure

The fundamental static problem takes the following form:

$$[K]\{d\} = \{P\} \quad (16)$$

In the above equation the overall stiffness matrix is expressed as K, while the generalized displacement as {d} and load vectors as {P}. The Gauss elimination method is employed for solving the equation applying boundary conditions. The global displacement vector {d} is the output of the solution. By using the above said equations the strains, force and moment resultants can be calculated at Gauss points. The nodal values can be obtained through extrapolation of these values.

2.2 Modeling of the cutout

The finite element code has the facilities for reshaping and relocating the size and position of cutouts as input. It is capable of producing a non-uniform finite element mesh across the cylindrical shell surface. The mesh refinement happens in steps. Ultimately, the element size near the cutout margins is gradually reduced. A 10 × 10 mesh is found to be suitable for all the problems considered in this study. Figure 4 illustrates a typical example of such a non-uniform mesh configuration. This process ensures that results converge for all the problems investigated in this study.

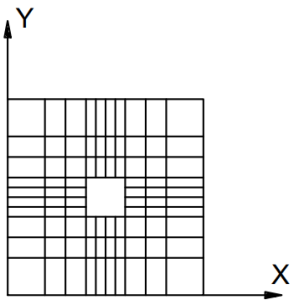

Fig. 4. Non-uniform mesh arrangement.

3. VALIDATION STUDY AND NUMERICAL PROCEDURE

A validation study is carried out to assess the suitability of the current technique. The current study compares its findings with those of Chang [22], Rossow and Ibrahimkhail [23] and Sinha et al. [24]. The current formulation is utilized to assess the central displacements of simply supported rectangular plates with one stiffener in each direction, ensuring zero curvature for the cylindrical shell. This is pretty similar to plates. The geometric and material properties considered for the validation study are: a = 30 in, b = 60 in, h =0.25, υ = 0.3, E = 30 x 10^6 lb/in^2. The dimensions for the x stiffener and y stiffener are considered as 0.5 × 5.0 in and 0.5 ×3.0 in, respectively. Table 1 presents a comparison of central displacements acquired through various methods. The data in Table 1 show that the current results match well with the previous ones. The aim of this comparison is to validate

the accuracy of the static formulations in the present finite element code for stiffened cylindrical shell with cutout. The cylindrical shell has been converted to plate considering $\frac{1}{R_x} = \frac{1}{R_y} = 0$ or $R_x = R_y = \infty$.

Table 1. Comparison of central deflection (in inches x103) for a rectangular stiffened plate.

Source	Distributed Load (10.0 lb/in²)		Central Concentrated Load (1.0 kip)	
	Concentric	Eccentric	Concentric	Eccentric
Chang [22]	24.077	8.996	3.464	1.246
Rossow and Ibrahimkhail [23]	24.075	8.850	3.464	1.270
Sinha et al. [24]	24.075	9.322	3.464	1.284
Present method	24.011	8.905	3.492	1.313

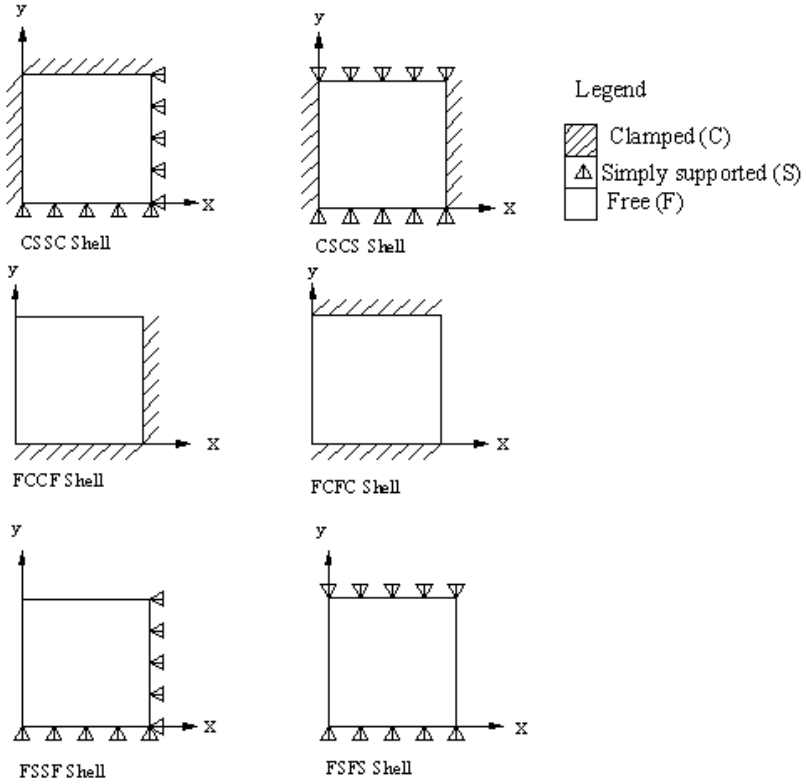

Fig. 5. Boundary conditions arrangement.

The location of cutout considered for the present study is concentric on the shell structure. The size of the cutout is taken 20% of the size of the shell panel [25]. The shell panel as well as cutout is taken as square in plan. The stiffeners are placed along the cutout periphery and extended up to the shell surface. The first order shear deformation theory for thin shells is used for present method. The cylindrical shell used in the present study incorporates the geometric shapes as: a/h = 100, h/R_y = 1/300, h/R_x = 0 and material properties as: E_{11}/E_{22} = 25, G_{12}/E_{22} = 0.5, G_{23}/E_{22} = 0.2, G_{13}/E_{22} = 0.5, ρ= 100 N-sec²/m⁴, $\nu_{12} = \nu_{21}$ = 0.25. Based on the validation results, the present study addressed further problems concerning the static responses of composite cylindrical shell with cutout constructed from multilayered graphite-epoxy. A laminate ply in an anti-symmetric angle configuration is chosen with stacking sequence $(\theta/-\theta)_n$ and θ varies from 15 to 75 degrees in increments of 15 degrees. Orthotropic shells i.e. 0 degree and 90 degree orientations are also incorporated to examine the effects of changes in lamination angle on deflection and stress resultants. The n value is taken as 1, 2 and 5. The study also provides a detail description of the effects of number of layers on its performance. For the analysis, laminated cylindrical stiffened shell with cutout is considered with variations in layer numbers: two, four and ten layers. This study offers comprehensive knowledge

regarding the static behavior of the shells under various boundary conditions. Figure 5 shows a diagrammatic representation of the boundary conditions taken for the analysis. The boundary conditions considered for analysis are CSSC, CSCS, FCCF, FCFC, FSSF and FSFS. Here, the boundary conditions are designated as C means clamped, S means simple supported and F means freely supported. The boundary conditions are taken in a counter clock wise orientation from the vertical axis. For example CSCS shell, the shell is clamped along x = 0, simple supported along y = 0, clamped along x = a and simple supported along y = b. The present study is grouped into three categories according to the boundary conditions. Similar type of boundary constraints with different orientation are taken in the same group, such as CSCS and CSSC are taken in group A, FCFC and FCCF are taken as group B, FSFS and FSSF are taken as group C. The main group is also divided into subgroups 1 and 2 for simplicity in identification.

4. RESULTS AND DISCUSSION

The dimensionless measurements of maximum downward deflection and stress resultants under distributed load for laminated composite stiffened cylindrical shells with cutout at six boundary conditions are presented in Table 2 to Table 14. The geometry and material parameters are chosen as: a/b = 1, a/h = 100, $a^{/}/b^{/} = 1$, h/R_y = 1/300, h/R_x = 0, E_{11}/E_{22} = 25, G_{12}/E_{22}= 0.5, G_{23}/E_{22} = 0.2, G_{13}/E_{22} = 0.5, $\nu_{12} = \nu_{21}$ = 0.25. The location of maximum dimensionless downward deflection is presented within the parentheses $(\bar{x}, \bar{y})$. Values marked with an asterisk indicate the lowest values identified from each boundary condition in these tables. Additionally, the study identifies the positions of the nodes $(\bar{x}, \bar{y})$ where the values are calculated and the same is reported in the Tables. The tables mainly contain detailed information regarding downward deflection, tensile and compressive in-plane forces, bending moments and twisting moments. Deflection in upward direction, tensile in-plane forces, hogging moments and in-plane shear forces that cause the shell element to rotate counterclockwise are considered as positive for the present study. Only the converged results are shown in all the cases. This study is essential for understanding the behavior of the shell under different shell actions. The performance of each shell combinations are ranked from 1 to 6 based on their stress resultants with consideration given solely to the anti-symmetric angle ply laminate configurations (not considered for orthotropic shells). The highest position is given to the shell structure that has the lowest downward deflection and lowest static stress resultant values. This offers a clear comparison of the relative responses of the shell.

4.1 Performance assessment of the shell under distinct boundary conditions for non-dimensional downward deflection

The maximum non-dimensional downward deflections under distinct boundary conditions for the shell are shown in Table 2. The dimensionless downward deflection table suggests that under all combinations of boundary conditions Group C shows maximum downward deflections. This primarily occurs because Group C shells have less restraint than other two groups of boundary conditions. Group C still shows the maximum deflection, even though both Group B and Group C have the same number of free edges. The primary reason for this is the clamped support present in Group B. This observation suggests that increasing the number of restraints leads to greater stability and rigidity. More restraint results in reduced deflection in the structure. The findings in Table 2 also indicate that the greatest downward deflection occurs at the free edges of a shell without any support. Upon comparing among the sub-groups, the static deflection table shows that subgroup 2 presents the maximum downward deflections. This occurs despite an increase in the number of degrees of freedom. A clear pattern is not found for subgroups - A1 and A2. That means deflection not only depends on the number of restraints present in the structure, but also on the position of the restraints within the structure. The structure becomes notably stiffer for the case when two opposite edges of a shell are left free than a shell with two adjacent free edges. This implies that shells with arrangements FCCF and FSSF show the highest downward deflections among their subgroup. Thus, maintaining a constant number of support constraints has a significant impact on the maximum deflection. This impact is particularly noticed at the time for free edges are present on the structural arrangement of

individual edge conditions. In the context of comparing Group B2 and Group C2 elements, it appears that for Group C2 has the higher downward deflection.

4.2 Performance assessment of the shell under distinct lamination angles for non-dimensional downward deflection

Lamination angles play a crucial role in calculating the downward deflections. It is observed from the Table 2 that under FCFC shell configuration, a lamination angle of $(15/-15)_5$ exhibit a lower value of deflection followed by CSCS with lamination angle $(45/-45)_5$ and CSSC with lamination angle $(30/-30)_5$ respectively. Table 2 also suggests that a lower angle ply lamination is a better choice than higher angle ply lamination. A close observation of the deflection table for Group A shows that for lamination angles up to $(30/-30)_5$, CSSC shells exhibit lesser deflections. However, beyond this range, CSCS shells show lesser deflection. So, for higher lamination angle CSCS shells are preferred. This preference indicates that the CSCS boundary condition is more suitable for resisting the stresses and strains associated with higher lamination angles. This is mainly due to its specific fiber orientation arrangement. For the other subgroup, deflections increase for Case 2 compared to Case 1. This is true for all lamination angles.

4.3 Performance assessment of the shell under number of lamination layers for non-dimensional downward deflection

A thorough examination of Table 2 reveals that as the number of lamination layers increases, the deflections decrease for all the boundary conditions. That means a ten-layer anti-symmetric laminates consistently outperform over both four-layer and two-layer angle ply laminates. This trend indicates that adding more number of layers to the laminate configuration leads to improved structural characteristics and overall effectiveness.

4.4 Comparative study of different shell actions under different boundary conditions

In the current study, an effort is also undertaken to compare the relative performance of anti-symmetric angle-ply laminated shell under six distinct boundary conditions. From each of subgroup the best combination is selected. As a result, six combinations are identified for all positive and negative values of downward deflection, in-plane forces, in-plane shear, bending moments and twisting moments separately. These combinations are detailed in ascending order of their magnitude in Table 15 and Table 16. For example, it is observed from the table that the lowest and highest values for tensile in-plane forces are observed in FCFC configuration with a lamination angle of (15/-15) and FCCF configuration with a lamination angle of $(15/-15)_5$ respectively. Hence for tensile in-plane forces, the FCFC configuration with a lamination angle of (15/-15) appears first in Table 15. The non-dimensional coordinates for the six combinations are also presented in the same tables. Arranging the different boundary conditions in order of their rank according to various shell actions can assist a practicing designer to select particular shell structure among multiple options. The results presented in Tables 15 and 16 clearly demonstrate that a shell that performs well for one type of shell action may not necessarily be the best choice for the other type of shell action. The $(15/-15)_5$ shell with FCFC boundary condition appears first for downward deflection but does not perform well in most other cases, except for in-plane shear and clockwise twisting moment.

The results can be better understood by counting how often each shell option appears the best among 13 different shell actions. From Tables 15 and 16, considering only the best condition, it is observed that FCFC boundary conditions appears first position in 9 times, while CSCS boundary conditions appears first position in 4 times. However, considering the number of layers, the ten-layer laminate appears first position in 8 times, while the four-layer laminate appears first position in 3 times, and the two-layer laminate appears first position in 2 times. Considering the lamination angle, the 15° anti-symmetric angle-ply structure appears first position in 8 times, the 75° laminate structure appears first position in 3 times, and the 30° and 60° laminates each appears first position in once. Therefore, it is evident that relying solely on deflection-based comparative studies may not fully sufficient for the overall

performance of the shells. However, taking the maximum probable shell structure that is the $(15/-15)_5$ shell with FCFC boundary conditions appears first in only 4 out of the 13 shell actions.

A thorough study taking all the combinations of Tables 15 and 16, ten-layer laminates appear 54 times out of a total of 78 possibilities. Meanwhile, the $(15/-15)_5$ angle ply appears 24 times, and the $(75/-75)_5$ angle ply appears 18 times. Based on this, the authors choose the top two combinations that are ten-layer FCFC shell and ten-layer CSCS shell for further analysis through a relative performance matrix. A characteristic relative performance matrix is depicted in Table 17. The primary goal of this work is to assist design engineers for selecting the optimal choice between two shells. This will be achieved by utilizing weighting factors derived from the data provided in the relative performance matrix. A relative performance matrix is developed based on the results presented in Tables 2-14. Table 17 compares the shells according to the following rules:

Assign a value of 1 to denote superiority and 0 to denote inferiority in the combination.

Assign the number 1 to both combinations in the case if the value of the shell action is not more than 10 percent.

From Table 17, it is found that ten layer CSCS shell action gets 7 points while ten layer FCFC shell action gets 4 points out of 13 shell actions.

5. CONCLUSIONS

Based on the analysis, the following conclusions are drawn:

1. It is observed that the FSSF and FCFC shells exhibit the highest and lowest downward deflections among all combinations of boundary conditions.
2. The maximum deflection decreases when more restraints are attached at the boundary conditions.
3. CSCS shells are preferred for higher lamination angles.
4. A ten-layer anti-symmetric laminate demonstrates superior performance compared to both four-layer and two-layer angle ply laminates.
5. Six combinations are identified for positive and negative values from all three groups in ascending order of magnitude that will help a practicing engineer in designing such shell structures.

Table 2. Maximum dimensionless downward deflections $(-\bar{w})$ x10^4 values.

Lamination (Number of layer and degree)	Boundary conditions					
	Group-A		Group-B		Group-C	
	A1	A2	B1	B2	C1	C2
	CSCS	CSSC	FCFC	FCCF	FSFS	FSSF
0	-4.0481 (05,0.6)	-3.6057 (0.65,0.4)	-0.68087 (1.0,0.5)	-18.220 (0.25,1.0)	-8.6330 (0.35,0.5)	-19.954 (0.25,1.0)
(15/-15)	-3.3361 (0.7,0.25)	-3.1096 (0.7,0.25)	-0.94990 (0,0.5)	-14.199 (0.3,1.0)	-7.8582 (0.25,0.5)	-17.095 (0.25,1.0)
$(15/-15)_2$	-3.0033 (0.5,0.4)	-2.5108 (0.7,0.3)	-0.91554 (0,0.5)	-12.945 (0.3,1.0)	-7.3947 (0.35,0.5)	-14.942 (0.3,1.0)
$(15/-15)_5$	-2.9529 (0.5,0.6)	-2.3867 (0.7,0.3)	-0.90650* (0,0.5)	-12.738 (0.3,1.0)	-7.2921 (0.35,0.5)	-14.429 (0.3,1.0)
(30/-30)	-2.5418 (0.25,0.8)	-2.5815 (0.75,0.2)	-2.5304 (0,0.5)	-12.242 (0.3,1.0)	-7.5674 (0,0.5)	-13.630 (0.3,1.0)
$(30/-30)_2$	-1.9909 (0.5,0.4)	-1.8741 (0.7,0.3)	-2.3906 (0,0.5)	-9.8415 (0.3,1.0)	-7.0561 (0.3,0.5)	-10.973 (0.3,1.0)
$(30/30)_5$	-1.9559 (0.5,0.6)	-1.7772* (0.7,0.3)	-2.3564 (0,0.5)	-9.3720 (0.3,1.0)	-6.9547 (0.3,0.5)	-10.700* (0.7,1.0)
(45/-45)	-1.9535	-2.5194	-6.2503	-10.872	-11.133	-13.364

	(0.25,0.8)	(0.75,0.2)	(1.0,0.5)	(0,0.5)	(1.0,0.5)	(0,0.5)
$(45/-45)_2$	-1.7425 (0.5,0.6)	-1.9627 (0.7,0.3)	-5.8740 (1.0,0.5)	-9.3068 (0,0.5)	-10.386 (1.0,0.5)	-11.462 (0,0.5)
$(45/-45)_5$	-1.7173* (0.5,0.4)	-1.8701 (0.7,0.3)	-5.7675 (0,0.5)	-8.9958* (0,0.5)	-10.231 (0,0.5)	-11.051 (0,0.5)
(60/-60)	-2.1733 (0.5,0.4)	-3.2909 (0.8,0.25)	-8.8854 (0,0.5)	-15.952 (0,0.55)	-14.549 (0,0.5)	-18.772 (0,0.5)
$(60/-60)_2$	-2.0491 (0.5,0.6)	-2.5089 (0.7,0.3)	-8.6529 (0,0.5)	-14.140 (0,0.55)	-13.954 (0,0.5)	-16.762 (0,0.5)
$(60/-60)_5$	-2.0176 (0.5,0.6)	-2.4329 (0.6,0.4)	-8.5572 (0,0.5)	-13.705 (0,0.55)	-13.795 (0,0.5)	-16.274 (0,0.5)
(75/-75)	-2.7137 (0.55,0.4)	-3.9709 (0.75,0.2)	-9.6281 (1.0,0.65)	-18.160 (0,0.65)	-5.5352* (1.0,0.3)	-24.004 (0,0.55)
$(75/-75)_2$	-2.5292 (0.5,0.4)	-3.2086 (0.7,0.3)	-9.2869 (1.0,0.5)	-16.862 (0,0.6)	-17.375 (1.0,0.5)	-22.575 (0,0.5)
$(75/-75)_5$	-2.4861 (0.5,0.6)	-3.0800 (0.6,0.4)	-9.2888 (1.0,0.5)	-16.564 (0,0.6)	-17.306 (1.0,0.5)	-22.282 (0,0.5)
90	-3.1520 (0.5,0.6)	-3.7696 (0.6,0.4)	-8.9224 (0,0.5)	-20.823 (0,0.65)	-20.797 (1.0,0.5)	-29.869 (0,0.55)

Table 3. Maximum dimensionless in-plane tensile forces ($+\overline{N_x}$) values.

Lamination (Number of layer and degree)	**Boundary conditions**					
	Group-A		**Group-B**		**Group-C**	
	A1	**A2**	**B1**	**B2**	**C1**	**C2**
	CSCS	**CSSC**	**FCFC**	**FCCF**	**FSFS**	**FSSF**
0	0.53438 (0,0.5)	0.35693 (0,0.4)	0.046396 (0.5,0.3)	2.3672 (0.2,1.0)	0.13014 (0,0.2)	2.0244 (0.2,1.0)
(15/-15)	1.1482 (0,0.3)	0.86460 (0,0.3)	0.040325* (0,0.9)	2.2008 (0.2,1.0)	0.40156 (0.9,0)	1.9982 (0.2,1.0)
$(15/-15)_2$	0.99403 (0,0.35)	0.72055 (0,0.3)	0.045368 (0,0.9)	1.9931 (0.2,1.0)	0.40780 (0.1,0)	1.7134 (1.0,0.9)
$(15/-15)_5$	0.95330 (1.0,0.6)	0.66202 (0,0.3)	0.046131 (0,0.9)	1.9567* (0.2,1.0)	0.40100* (0.1,0)	1.6744 (1.0,0.9)
(30/-30)	1.3297 (0,0.3)	0.87095 (0,0.3)	0.32125 (0,0.9)	2.6824 (0.1,1.0)	2.7743 (0.1,0)	3.1884 (0.4,1.0)
$(30/-30)_2$	1.1080 (0,0.3)	0.67856 (0,0.3)	0.32929 (0,0.9)	2.5905 (0.4,1.0)	2.6361 (0.1,0)	3.0925 (0.4,1.0)
$(30/30)_5$	1.0726 (0,0.3)	0.62472 (0,0.3)	0.32839 (0,0.9)	2.5685 (0.1,1.0)	2.5327 (0.1,0)	3.0408 (0.6,1.0)
(45/-45)	0.70889 (1.0,0.8)	1.4420 (1.0,0.1)	1.6275 (0,0.9)	4.0970 (0.1,1.0)	5.7171 (0.9,1.0)	5.7558 (1.0,0.9)
$(45/-45)_2$	0.52372 (1.0,0.8)	0.55400 (0,0.2)	1.5351 (1.0,0.1)	3.7652 (0.1,1.0)	5.4932 (0.1,0)	5.3030 (0.1,0)
$(45/-45)_5$	0.46973* (0,0.2)	0.48116* (0,0.2)	1.5096 (0,0.9)	3.6941 (0.1,1.0)	5.3764 (0.1,0)	0.51528* (0.1,0)
(60/-60)	1.1480 (0.9,1.0)	2.3143 (1.0,0.1)	4.8544 (0.5,0.65)	4.3956 (0.4,1.0)	10.022 (0,0.9)	8.7007 (1.0,0.9)
$(60/-60)_2$	1.0458 (0.5,0.6)	1.4603 (0.5,0.6)	4.8310 (0.5,0.65)	4.7607 (0.4,1.0)	9.8497 (0,0.9)	8.6965 (0,0.1)

$(60/-60)_5$	1.0681 (0.5,0.4)	1.4471 (0.5,0.6)	4.8189 (0.5,0.65)	4.8298 (0.4,1.0)	9.5800 (0,0.9)	9.0471 (0,0.1)
(75/-75)	1.9453 (0.1,0)	2.0268 (0.5,0.65)	4.0696 (0.5,0.65)	6.5806 (0.4,1.0)	8.3352 (1.0,0.1)	10.208 (0.4,1.0)
$(75/-75)_2$	1.1287 (0.5,0.6)	1.9633 (0.5,0.65)	3.9650 (0.5,0.65)	7.6350 (0.4,1.0)	7.2233 (1.0,0.1)	10.953 (0.4,1.0)
$(75/-75)_5$	1.1631 (0.5,0.4)	1.9609 (0.5,0.65)	3.9409 (0.5,0.35)	7.9351 (0.4,1.0)	6.5829 (1.0,0.1)	11.022 (0.4,1.0)
90	1.0161 (0.5,0.7)	0.75184 (0.5,0.7)	1.1031 (0.5,0.7)	8.6827 (0.4,1.0)	1.7259 (0.5,0.7)	12.865 (0.4,1.0)

Table 4. Maximum dimensionless in-plane compressive forces ($-\overline{N_x}$) values.

Lamination (Number of layer and degree)	**Boundary conditions**					
	Group-A		**Group-B**		**Group-C**	
	A1	**A2**	**B1**	**B2**	**C1**	**C2**
	CSCS	**CSSC**	**FCFC**	**FCCF**	**FSFS**	**FSSF**
0	-0.72376 (05,065)	-0.85226 (0.5,0.35)	-0.052023 (0.5,0.6)	-6.0337 (1.0,1.0)	-1.4463 (05,0.65)	-6.8365 (1.0,1.0)
(15/-15)	-0.91057* (0.5,0.35)	-0.65723* (0.5,0.35)	-0.34633* (0,0)	-8.8374 (0,1.0)	-3.8444 (0,0)	-9.7584 (0,1.0)
$(15/-15)_2$	-0.94191 (0.5,0.35)	-0.76113 (0.5,0.35)	-0.35095 (0,0)	-8.5746 (0,1.0)	-3.4877 (0,0)	-9..7635 (0,1.0)
$(15/-15)_5$	-0.94776 (0.5,0.35)	-0.78500 (0.5,0.35)	-0.35124 (0,0)	-8.3633* (0,1.0)	-3.3393* (0,0)	-9.7474* (0,1.0)
(30/-30)	-1.6955 (0.4,0.65)	-3.2739 (1.0,0)	-2.7055 (0,1.0)	-12.613 (0,1.0)	-12.534 (0,0)	-15.325 (0,1.0)
$(30/-30)_2$	-1.4751 (0.4,0.65)	-1.4512 (0.6,0.65)	-2.6486 (0,1.0)	-12.061 (0,1.0)	-11.975 (0,0)	-14.877 (0,1.0)
$(30/30)_5$	-1.4001 (0.4,0.65)	-1.4457 (0.6,0.65)	-2.6234 (0,1.0)	-11.845 (0,1.0)	-11.748 (0,0)	-14.871 (0,1.0)
(45/-45)	-2.6898 (0.4,0.6)	-7.3598 (1.0,0)	-9.3174 (0,1.0)	-20.291 (0,1.0)	-28.544 (0,1.0)	-27.324 (0,0)
$(45/-45)_2$	-2.4265 (0.4,0.6)	-2.5348 (0.6,0.6)	-8.7561 (1.0,0)	-18.333 (0,1.0)	-28.213 (1.0,0)	-26.371 (0,0)
$(45/-45)_5$	-2.3663 (0.6,0.4)	-2.5722 (0.6,0.6)	-8.6087 (0,1.0)	-17.925 (0,1.0)	-27.925 (0,1.0)	-26.388 (0,0)
(60/-60)	-2.8804 (0.4,0.4)	-9.6643 (1.0,0)	-9.9142 (0,0)	-26.099 (0,1.0)	-45.819 (0,1.0)	-39.235 (0,0)
$(60/-60)_2$	-2.6933 (0.65,0.4)	-2.6020 (0.35,0.5)	-9.2913 (0,1.0)	-21.726 (0,1.0)	-45.056 (0,1.0)	-41.046 (0,0)
$(60/-60)_5$	-2.6670 (0.35,0.6)	-2.6314 (0.35,0.4)	-9.1252 (0,1.0)	-20.777 (0,1.0)	-44.054 (0,1.0)	-42.107 (0,0)
(75/-75)	-2.7910 0.1,1.0)	-6.2510 (1.0,0)	-2.8335 (1.0,1.0)	-24.047 (1.0,1.0)	-40.239 (1.0,0)	-29.794 (1.0,1.0)
$(75/-75)_2$	-2.1222 (0.35,0.5)	-2.1987 (0.35,0.5)	-2.6478 (1.0,0)	-22.951 (1.0,1.0)	-34.542 (1.0,0)	-29.122 (0,0)
$(75/-75)_5$	-2.1164 (0.65,0.5)	-2.1789 (0.35,0.5)	-2.5869 (1.0,0)	-22.932 (1.0,1.0)	-31.607 (1.0,0)	-31.206 (0,0)
90	-1.1174 (0.5,0.6)	-1.8064 (0.5,0.4)	-0.60061 (0.5,0.6)	-20.389 (1.0,1.0)	-7.1853 (1.0,1.0)	-20.992 (1.0,1.0)

Table 5. Maximum dimensionless in-plane tensile forces ($+\overline{N_y}$) values.

Lamination (Number of layer and degree)	Boundary conditions					
	Group-A		Group-B		Group-C	
	A1	A2	B1	B2	C1	C2
	CSCS	CSSC	FCFC	FCCF	FSFS	FSSF
0	3.7045 (0.4,0.5)	3.2370 (0.4,0.4)	0 (0.55,0.5)	9.1259 (0.4,1.0)	7.4398 (0.4,0.5)	9.8513 (0.4,1.0)
(15/-15)	2.6226 (0.4,0.4)	1.9749 (0.4,0.4)	0 (0.55,0.5)	11.288 (0.1,1.0)	8.7167 (0.1,0)	9.3646 (0.1,1.0)
$(15/-15)_2$	1.8532 (0.4,0.5)	1.4391 (0.4,0.4)	0 (0.55,0.5)	10.658 (0.1,1.0)	8.4635 (0.1,0)	9.0944 (0.1,1.0)
$(15/-15)_5$	1.7908 (0,0.5)	1.2704 (0.4,0.4)	0 (0.55,0.5)	10.422 (0.1,1.0)	8.1742 (0.1,0)	9.0229 (0.1,1.0)
(30/-30)	2.3085 (0,0.3)	2.1153 (0.9,0)	0 (0.55,0.5)	11.556 (0.1,1.0)	9.3148 (0.1,0)	10.278 (0.1,1.0)
$(30/-30)_2$	2.0320 (0,0.3)	1.2499 (0,0.3)	0 (0.55,0.5)	10.908 (0.1,1.0)	8.9238 (0.1,0)	9.7854 (0.1,1.0)
$(30/30)_5$	1.9978 (0,0.7)	1.1824 (0,0.3)	0 (0.55,0.5)	10.750 (0.1,1.0)	8.6443 (0.1,0)	9.6980 (0.1,1.0)
(45/-45)	0.64076 (1.0,0.8)	1.3714 (0.9,0)	0 (0.55,0.5)	7.5296 (0.1,1.0)	6.9171 (0.9,1.0)	7.8052 (0.1,1.0)
$(45/-45)_2$	0.47537 (1.0,0.8)	0.50010 (0,0.2)	0 (0.55,0.5)	6.9707 (0.1,1.0)	6.7368 (0.1,0)	7.4445 (0.1,1.0)
$(45/-45)_5$	0.42805 (0,0.2)	0.43632 (0,0.2)	0 (0.55,0.5)	6.8535 (0.1,10)	6.6330 (0.1,0)	7.3722 (0.1,1.0)
(60/-60)	0.19767 (0.35,1.0)	0.50644 (1.0,0.1)	0.14061 (0.5,0.7)	4.1382 (0.1,1.0)	4.1015 (0.1,0)	4.6348 (0.1,1.0)
$(60/-60)_2$	0.064248 (0.3,1.0)	0.12271 (1.0,0.1)	0.16028 (0.5,0.7)	3.8195 (0.1,1.0)	4.1286 (0.1,0)	4.4223 (0.1,1.0)
$(60/-60)_5$	0.022808* (0,0)	0.030306* (1.0,0.1)	0.15849 (0.5,0.7)	3.7410 (0.1,1.0)	4.1208 (0.1,0)	4.3662* (0.1,1.0)
(75/-75)	0.18253 (0.6,0.5)	0.16808 (0.4,0.5)	0.10265 (0.4,0.5)	3.6229 (0.1,1.0)	9.2262 (1.0,0)	4.4279 (0.1,1.0)
$(75/-75)_2$	0.18172 (0.6,0.5)	0.15662 (0.4,0.5)	0.083189 (0.4,0.5)	3.4689 (0.1,1.0)	3.4048 (0.9,1.0)	4.3968 (0.1,1.0)
$(75/-75)_5$	0.18239 (0.4,0.5)	0.14979 (0.4,0.5)	0.078831* (0.4,0.5)	3.3922* (0.1,1.0)	3.4048* (0.9,1.0)	4.3674 (0.1,1.0)
90	0.69220 (0.65,0.5)	0.52028 (0.35,0.5)	0.21263 (0.6,0.5)	4.1579 (0.1,1.0)	3.6423 (0.9,1.0)	5.0668 (0.1,1.0)

Table 6. Maximum dimensionless in-plane compressive forces ($-\overline{N_y}$) values.

Lamination (Number of layer and degree)	Boundary conditions					
	Group-A		Group-B		Group-C	
	A1	A2	B1	B2	C1	C2
	CSCS	CSSC	FCFC	FCCF	FSFS	FSSF
0	-4.5583 (05,0.35)	-4.5050 (0.5,0.35)	-3.8935 (0.5,0.35)	-41.488 (0,1.0)	-30.472 (0,0)	-39.075 (0,1.0)
(15/-15)	-47.096 (0,1.0)	-5.7356 (1.0,0)	-4.5265 (0,1.0)	-47.096 (0,1.0)	-39.075 (0,0)	-42.033 (0,1.0)

$(15/-15)_2$	-3.8642 (0.5,0.35)	-3.7978 (0.5,0.35)	-4.5283 (0,1.0)	-45.877 (0,1.0)	-36.075 (0,0)	-40.845 (0,1.0)
$(15/-15)_5$	-3.8283 (0.5,0.35)	-3.7766 (0.5,0.35)	-4.5216 (0,1.0)	-45.429 (0,1.0)	-34.627 (0,0)	-40.499 (0,1.0)
(30/-30)	-2.7205 (0.3,0.5)	-8.8944 (1.0,0)	-8.3881 (0,1.0)	-43.581 (0,1.0)	-36.637 (0,0)	-41.271 (0,1.0)
$(30/-30)_2$	-2.6228 (0.3,0.5)	-3.4213 (0.6,0.7)	-8.1739 (0,1.0)	-42.775 (0,1.0)	-35.052 (0,0)	-40.353 (0,1.0)
$(30/30)_5$	-2.6000 (0.3,0.5)	-3.4315 (0.6,0.7)	-8.0951 (0,1.0)	-42.465 (0,1.0)	-34.240 (0,0)	-40.188 (0,1.0)
(45/-45)	-2.6181 (0.4,0.6)	-7.1770 (1.0,0)	-10.741 (0,1.0)	-35.088 (0,1.0)	-32.004 (1.0,1.0)	-38.445 (0,1.0)
$(45/-45)_2$	-2.4456 (0.4,0.6)	-2.7988 (0.6,0.6)	-10.107 (1.0,0)	-32.706 (0,1.0)	-31.516 (0,0)	-37.179 (0,1.0)
$(45/-45)_5$	-2.3965 (0.4,0.6)	-2.8228 (0.6,0.6)	-9.9693 (0,1.0)	-32.154 (0,1.0)	-31.383 (0,0)	-36.940 (0,1.0)
(60/-60)	-1.4788 (0.65,0.6)	-3.3872 (1.0,0)	-5.9982 (0,0)	-26.532 (0,1.0)	-24.512 (0,1.0)	-30.253 (0,1.0)
$(60/-60)_2$	-1.3652 (0.65,0.6)	-1.4895 (0.65,0.4)	-5.5303 (0,0)	-23.977 (0,1.0)	-24.539 (0,1.0)	-28.808 (0,10)
$(60/-60)_5$	-1.3459 (0.65,0.6)	-1.4581 (0.65,0.6)	-5.4239 (0,0)	-23.346 (0,1.0)	-24.462 (0,1.0)	-28.542 (0,1.0)
(75/-75)	-1.2608 (0.5,0.35)	-1.2501* (0.5,0.65)	-2.6546 (1.0,1.0)	-2.0035* (0,1.0)	-9.2261* (0,0)	-25.406 (0,1.0)
$(75/-75)_2$	-1.2467 (0.5,0.35)	-1.2621 (0.5,0.65)	-2.4670 (1.0,1.0)	-19.023 (0,1.0)	-19.821 (1.0,0)	-25.334 (0,1.0)
$(75/-75)_5$	-1.2435* (0.5,0.65)	-1.2699 (0.5,0.65)	-2.4180* (1.0,1.0)	-18.574 (0,1.0)	-19.636 (1.0,0)	-25.284* (0,1.0)
90	-2.3438 (05,0.65)	-2.4428 (05,0.65)	-2.4406 (0.5,0.35)	-19.199 (0,1.0)	-16.765 (1.0,1.0)	-23.621 (0,1.0)

Table 7. Maximum dimensionless anticlockwise in-plane shear ($+\bar{N}_{xy}$) values.

Lamination (Number of layer and degree)	**Boundary conditions**					
	Group-A		**Group-B**		**Group-C**	
	A1	**A2**	**B1**	**B2**	**C1**	**C2**
	CSCS	**CSSC**	**FCFC**	**FCCF**	**FSFS**	**FSSF**
0	0.86129 (0.9,0)	1.4238 (1.0,0)	0.064170 (0.45,0.7)	10.488 (0,1.0)	7.4319 (1.0,0)	10.658 (0,1.0)
(15/-15)	2.0869 (1.0,0)	3.9809 (1.0,0)	0.62297 (0,1.0)	17.514 (0,1.0)	11.017 (1.0,0)	16.563 (0,1.0)
$(15/-15)_2$	1.7312 (0.95,0)	2.7582 (1.0,0)	0.61942 (0,1.0)	16.971 (0,1.0)	11.306 (1.0,0)	16.442 (0,1.0)
$(15/-15)_5$	1.8009 (0.1,1.0)	2.4251 (1.0,0)	0.61852* (0,1.0)	16.663 (0,1.0)	11.594 (1.0,0)	16.403* (0,1.0)
(30/-30)	3.7628 (0,1.0)	6.3347 (1.0,0)	3.6195 (0,1.0)	23.448 (0,1.0)	18.385 (1.0,0)	24.117 (0,1.0)
$(30/-30)_2$	2.3558 (0.1,1.0)	3.5531 (1.0,0)	3.4898 (0,1.0)	22.449 (0,1.0)	17.892 (0,1.0)	23.328 (0,1.0)
$(30/30)_5$	2.4126	2.8829	3.4535	22.125	17.951	23.233

	(0.1,1.0)	(1.0,0)	(0,1.0)	(0,1.0)	(0,1.0)	(0,1.0)
(45/-45)	4.0167 (0,1.0)	7.6878 (1.0,0)	8.6077 (0,1.0)	27.038 (0,1.0)	26.918 (0,1.0)	31.549 (0,1.0)
$(45/-45)_2$	2.8353 (0,1.0)	4.0496 (1.0,0)	8.0730 (1.0,0)	24.869 (0,1.0)	25.692 (1.0,0)	30.474 (0,1.0)
$(45/-45)_5$	2.6044 (0,1.0)	3.1891 (1.0,0)	7.9546 (0,1.0)	24.397 (0,1.0)	25.407 (0,1.0)	30.346 (0,1.0)
(60/-60)	1.9675 (1.0,0)	6.0777 (1.0,0)	5.8210 (0,1.0)	25.000 (0,1.0)	26.332 (0,1.0)	28.983 (0,1.0)
$(60/-60)_2$	1.7487 (0,1.0)	3.2667 (1.0,0)	5.5539 (0,1.0)	22.481 (0,1.0)	24.670 (0,1.0)	27.913 (0,1.0)
$(60/-60)_5$	1.7024 (0,1.0)	2.5853 (1.0,0)	5.5012 (0,1.0)	21.917 (0,1.0)	24.124 (0,1.0)	27.893 (0,1.0)
(75/-75)	1.3221 (0,0.9)	2.9218 (1.0,0)	1.8278 (0.4,0.6)	17.282 (0,1.0)	1.7139* (1.0,0.1)	22.864 (0,1.0)
$(75/-75)_2$	1.3023* (0.6,0.4)	1.9462 (1.0,0)	1.7238 (0.4,0.6)	16.774 (0,1.0)	19.950 (1.0,0)	23.627 (0,1.0)
$(75/-75)_5$	1.3265 (0.4,0.6)	1.6731* (1.0,0)	1.6599 (0.6,0.4)	16.507* (0,1.0)	19.514 (1.0,0)	23.912 (0,1.0)
90	1.1441 (0.4,0.65)	1.0859 (0.6,0.35)	0.77268 (0.4,0.65)	14.310 (0,1.0)	13.038 (1.0,0)	17.701 (0,1.0)

Table 8. Maximum dimensionless clockwise in-plane shear ($-\bar{N}_{xy}$) values.

Lamination (Number of layer and degree)	**Boundary conditions**					
	Group-A		**Group-B**		**Group-C**	
	A1	**A2**	**B1**	**B2**	**C1**	**C2**
	CSCS	**CSSC**	**FCFC**	**FCCF**	**FSFS**	**FSSF**
0	-0.86130 (0.1,0)	-1.1584 (0.1,0)	-0.064172 (0.55,0.7)	-1.8162 (0.9,0.9)	-7.4331 (0,0)	-8.7332 (0,0)
(15/-15)	-1.7662 (0.1,0.1)	-2.0114 (0.1,0.1)	-0.64118 (0,0)	-4.6793 (1.0,1.0)	-13.472 (0,0)	-13.070 (0,0)
$(15/-15)_2$	-1.8390 (0.1,0)	-2.0938 (0.1,0)	-0.63084 (0,0)	-3.939 (1.0,1.0)	-12.567 (0,0)	-12.768 (0,0)
$(15/-15)_5$	-1.8497 (0.1,0)	-2.1357 (0.1,0)	-0.62341* (0,0)	-3.7238 (1.0,1.0)	-12.101* (0,0)	-12.705* (0,0)
(30/-30)	-2.5176 (0.1,0.1)	-2.5563 (0.1,0.1)	-3.6626 (0,0)	-12.028 (1.0,1.0)	-19.857 (0,0)	-19.188 (0,0)
$(30/-30)_2$	-2.4778 (0.1,0)	-2.4735 (0.1,0)	-3.5038 (0,0)	-10.096 (1.0,1.0)	-18.779 (0,0)	-18.120 (0,0)
$(30/30)_5$	-2.4582 (0.1,0)	-2.4629 (0.1,0)	-3.4588 (0,0)	-9.7262 (1.0,1.0)	-18.316 (0,0)	-17.876 (0,0)
(45/-45)	-2.8315 (1.0,1.0)	-2.7449 (0,0)	-8.5609 (1.0,1.0)	-13.224 (1.0,1.0)	-26.500 (1.0,1.0)	-26.744 (0,0)
$(45/-45)_2$	-2.4971 (0.1,0)	-2.4872 (0.1,0)	-8.0543 (1.0,1.0)	-11.606 (1.0,1.0)	-25.611 (0,0)	-24.835 (0,0)
$(45/-45)_5$	-2.4739 (0.05,0)	-2.4465 (0.1,0)	-7.9473 (0,0)	-11.340 (1.0,1.0)	-25.385 (0,0)	-24.366 (0,0)
(60/-60)	-2.2096 (1.0,1.0)	-2.0682 (0,0)	-6.1096 (0,0)	-8.7933 (0,0)	-23.968 (0,0)	-25.709 (0,0)

$(60/-60)_2$	-1.8180 (1.0,0.9)	-1.9815 (1.0,0.9)	-5.6139 (0,0)	-8.0941 (0,0)	-23.626 (0,0)	-24.212 (0,0)
$(60/-60)_5$	-1.7372 (1.0,0.9)	-1.9637 (1.0,0.9)	-5.5197 (0,0)	-7.8839 (0,0)	-23.716 (0,0)	-23.776 (0,0)
(75/-75)	-1.9319 (0,0)	-2.2219 (0,0)	-1.4393 (0.6,0.6)	-3.0852 (0,0.9)	-8.1809 (1.0,0)	-22.005 (0,0)
$(75/-75)_2$	-1.3781 (0,0)	-1.5393 (0,0)	-1.5177 (0.4,0.4)	-3.0798 (0,0.9)	-18.752 (1.0,1.0)	-21.395 (0,0)
$(75/-75)_5$	-1.3481* (0.6,0.6)	-1.3545* (0.4,0.4)	-1.5774 (0.4,0.4)	-3.0514* (0,0.9)	-19.039 (1.0,1.0)	-21.259 (0,0)
90	-1.1441 (0.6,0.65)	-1.1987 (0.4,0.35)	-0.77275 (0.6,0.65)	-2.1821 (0.7,0.9)	-13.039 (1.0,1.0)	-16.201 (0,0)

Table 9. Maximum dimensionless hogging moments $(+\bar{\mathbf{M}}_{\mathbf{x}})$ x 10^2 values.

Lamination (Number of layer and degree)	**Boundary conditions**					
	Group-A		**Group-B**		**Group-C**	
	A1	**A2**	**B1**	**B2**	**C1**	**C2**
	CSCS	**CSSC**	**FCFC**	**FCCF**	**FSFS**	**FSSF**
0	0.40206 (0,0.3)	0.37178 (0,0.3)	0.0085339 (0.4,0.2)	2.1238 (0,1.0)	0.14748 (0.4,0.2)	2.3571 (0,1.0)
(15/-15)	0.58742 (1.0,0.15)	0.21481* (1.0,0)	0.043974 (0,1.0)	2.2062 (0,1.0)	0.61362 (0,1.0)	2.6516 (0,1.0)
$(15/-15)_2$	0.44756 (0,0.8)	0.25769 (0,0.3)	0.039772* (0,1.0)	1.8635 (0,1.0)	0.35129 (0,1.0)	2.2533 (0,1.0)
$(15/-15)_5$	0.39304* (0,0.8)	0.29070 (0,0.3)	0.041316 (0.7,0)	1.6426* (0,1.0)	0.17327* (0,1.0)	1.9954* (0,1.0)
(30/-30)	0.83432 (0,0.9)	0.84393 (1.0,0)	0.53658 (0,1.0)	4.5347 (0,1.0)	2.6305 (0,1.0)	5.0315 (0,1.0)
$(30/-30)_2$	0.69015 (0,0.8)	0.36264 (0,0.3)	0.39428 (0,1.0)	3.1572 (0,1.0)	1.8164 (0,1.0)	3.7895 (0,1.0)
$(30/30)_5$	0.62372 (0,0.8)	0.45765 (0,0.2)	0.28170 (0,1.0)	2.2878 (0,1.0)	1.1854 (1.0,0)	2.9176 (0,1.0)
(45/-45)	1.2208 (0,0.9)	1.8010 (1.0,0)	2.4050 (0,1.0)	8.4821 (0,1.0)	7.1149 (0,1.0)	9.3648 (0,1.0)
$(45/-45)_2$	1.1074 (0,0.8)	0.71487 (0,0.3)	1.7193 (1.0,0)	6.8226 (0,1.0)	5.1643 (0,1.0)	7.2627 (0,1.0)
$(45/-45)_5$	1.0227 (0,0.8)	0.86875 (0,0.3)	1.2234 (0,1.0)	5.4719 (0,1.0)	3.6235 (0,1.0)	5.5135 (0,1.0)
(60/-60)	1.8848 (1.0,0.2)	2.3613 (1.0,0)	3.0661 (0,1.0)	11.766 (0,1.0)	11.792 (0,1.0)	12.810 (0,1.0)
$(60/-60)_2$	1.8407 (0,0.8)	1.3746 (0,0.7)	2.5264 (0,1.0)	10.039 (0,1.0)	8.1656 (0,1.0)	10.513 (0,1.0)
$(60/-60)_5$	1.7082 (0,0.8)	1.5187 (0,0.3)	1.9898 (0,1.0)	8.5524 (0,1.0)	5.5959 (0,1.0)	8.4707 (0,1.0)
(75/-75)	2.7700 (0,0.8)	1.9944 (0,0.8)	1.5825 (0.4,0.6)	11.010 (0,1.0)	1.4223 (1.0,0.9)	13.343 (0,1.0)
$(75/-75)_2$	2.6545 (1.0,0.2)	2.2793 (0,0.5)	1.5380 (0.6,0.7)	9.1243 (0,1.0)	8.3977 (1.0,0)	10.434 (0,1.0)
$(75/-75)_5$	2.5825 (1.0,0.3)	2.4143 (0,0.5)	1.5670 (0.4,0.3)	7.8939 (0,1.0)	4.5604 (1.0,0)	8.4057 (0,1.0)

90	3.2075 (0,0.2)	3.1502 (0,0.3)	1.8206 (0.6,0.7)	5.9786 (1.0,1.0)	2.5913 (0.4,0.3)	6.0377 (0,1.0)

Table 10. Maximum dimensionless sagging moments ($-\bar{M}_x$) x 10^2 values.

Lamination (Number of layer and degree)	Boundary conditions					
	Group-A		Group-B		Group-C	
	A1	A2	B1	B2	C1	C2
	CSCS	CSSC	FCFC	FCCF	FSFS	FSSF
0	-0.13930 (0.7,0.8)	-0.14319 (0.7,0.2)	-0.009979 (0.7,0.7)	-0.80653 (0.2,1.0)	-0.19529 (0.3,0.8)	-0.87289 (0.2,1.0)
(15/-15)	-0.23992 (0.7,0.2)	-0.21284 (0.1,0.2)	-0.028163 (0.5,0.2)	-0.63311 (0.2,1.0)	-0.82130 (0,0)	-0.78422 (0,0)
$(15/-15)_2$	-0.18476 (0.7,0.2)	-0.17871 (0.1,0.2)	-0.02100* (0.7,0.7)	-0.49555 (0.2,1.0)	-0.34141 (0,0)	-0.55400 (0.2,1.0)
$(15/-15)_5$	-0.17505* (0.3,0.8)	-0.17348* (0.7,0.2)	-0.022015 (0.1,0.5)	-0.46269 (0.2,1.0)	-0.29656* (0.3,0.8)	-0.50554* (0.2,1.0)
(30/-30)	-0.50277 (0.1,0.2)	-0.49773 (0.1,0.2)	-0.41320 (0,0)	-0.95943 (0.1,1.0)	-2.7424 (0,0)	-2.5316 (0,0)
$(30/-30)_2$	-0.36789 (0.1,0.2)	-0.35731 (0.1,0.2)	-0.12789 (0.1,0.5)	-0.65851 (0.1,1.0)	-0.80848 (0,0)	-0.73867 (0.1,1.0)
$(30/30)_5$	-0.30919 (0.2,0.2)	-0.3009 (0.2,0.2)	-0.14448 (0.1,0.5)	-0.45327* (0.1,1.0)	-0.44793 (0.7,0.3)	-0.53504 (0.1,1.0)
(45/-45)	-0.81354 (0.1,0.1)	-0.80850 (0.1,0.1)	-1.6776 (1.0,1.0)	-1.6207 (1.0,1.0)	-5.8193 (1.0,1.0)	-5.7148 (0,0)
$(45/-45)_2$	-0.58626 (0.2,0.2)	-0.60265 (0.2,0.2)	-0.36107 (0.9,0.5)	-1.1235 (0.1,1.0)	-1.1755 (0,0)	-1.1181 (0.1,1.0)
$(45/-45)_5$	-0.47346 (0.2,0.2)	-0.48597 (0.2,0.2)	-0.40796 (0.9,0.5)	-0.85401 (0.1,1.0)	-0.63747 (0.9,0.5)	-0.80153 (0.1,1.0)
(60/-60)	-1.0546 (0.8,0.8)	-1.0931 (0.8,0.8)	-1.7473 (0,0)	-2.9486 (0,0)	-8.4113 (0,0)	-9.2169 (0,0)
$(60/-60)_2$	-0.78304 (0.8,0.8)	-0.92781 (0.8,0.8)	-0.55486 (0,0.9)	-2.0221 (0,0.9)	-1.7472 (1.0,1.0)	-2.1291 (0,0.9)
$(60/-60)_5$	-0.64441 (0.2,0.2)	-0.80956 (0.8,0.8)	-0.44246 (0,0.9)	-1.6904 (0,0.9)	-1.1070 (0,0.9)	-1.6772 (0,0.9)
(75/-75)	-1.3279 (0,0)	-1.5529 (0.2,0.1)	-0.56480 (0.4,0.4)	-2.5973 (0.7,0.9)	-11.596 (1.0,1.0)	-14.205 (0,0)
$(75/-75)_2$	-0.98420 (0.2,0.1)	-1.3044 (0.8,0.8)	-0.32771 (0.35,0.5)	-2.1063 (0.3,1.0)	-4.4814 (1.0,1.0)	-5.5403 (0,0)
$(75/-75)_5$	-0.82768 (0.7,0.7)	-1.3775 (0.8,0.2)	-0.33419 (0.65,0.5)	-2.1123 (0.4,1.0)	-0.99068 (1.0,0.1)	-1.8906 (0.8,0.9)
90	-0.99577 (0.3,0.7)	-1.8924 (0.8,0.2)	-0.50002 (0.7,0.5)	-3.6574 (0.4,1.0)	-0.96384 (0.3,0.5)	-3.5390 (0.4,1.0)

Table 11. Maximum dimensionless hogging moments ($+\bar{M}_y$) x 10^2 values.

Lamination (Number of layer and degree)	Boundary conditions					
	Group-A		Group-B		Group-C	
	A1	A2	B1	B2	C1	C2
	CSCS	CSSC	FCFC	FCCF	FSFS	FSSF
0	0.56549 (0.1,0.6)	2.3976 (0.7,1.0)	0.49845 (0.3,0)	2.7065 (0,0.9)	2.4007 (0,0.1)	2.9439 (0,0.1)
(15/-15)	1.4167 (1.0,0)	2.6137 (1.0,0)	0.53535 (0,1.0)	8.8784 (0,1.0)	7.2976 (0,1.0)	9.9644 (0,1.0)
$(15/-15)_2$	0.92349 (0,0.85)	1.1422 (0.2,1.0)	0.49085* (0,1.0)	4.2442 (0,1.0)	4.2203 (0,1.0)	6.0478 (0,1.0)
$(15/-15)_5$	0.72803 (0,0.8)	1.1715 (0.2,1.0)	0.51384 (0.7,0)	2.7333 (0,0)	2.1192 (0,1.0)	3.4618 (0,1.0)
(30/-30)	1.4596	2.4050	1.5584	8.6595	7.5814	9.9099

	(0,1.0)	(1.0,0)	(0,1.0)	(0,1.0)	(0,1.0)	(0,1.0)
$(30/-30)_2$	1.2479 (0,0.8)	0.81511 (0.2,1.0)	1.1677 (0,1.0)	5.8127 (0,1.0)	5.3421 (0,1.0)	7.5120 (0,1.0)
$(30/30)_5$	1.1428 (0,0.8)	0.78053 (0.2,1.0)	0.84920 (0,1.0)	3.5663 (0,1.0)	3.5464 (1.0,0)	5.3015 (0,1.0)
(45/-45)	0.94225 (0,0.9)	1.7574 (1.0,0)	2.5426 (0,1.0)	7.5876 (0,1.0)	7.3373 (0,1.0)	8.5525 (0,1.0)
$(45/-45)_2$	0.94712 (0,0.8)	0.56958 (0,0.3)	1.8383 (1.0,0)	6.2757 (0,1.0)	5.4768 (0,1.0)	6.7859 (0,1.0)
$(45/-45)_5$	0.87918 (0,0.8)	0.73319 (0,0.3)	1.3474 (1.0,0)	5.0006 (0,1.0)	3.9622 (0,1.0)	5.1143 (0,1.0)
(60/-60)	0.56610 (1.0,0.2)	0.79136 (1.0,0)	1.5403 (0,1.0)	4.6541 (0,1.0)	4.8902 (0,1.0)	4.9512 (0,1.0)
$(60/-60)_2$	0.58333 (0,0.8)	0.43473 (0,0.7)	1.2411 (0,1.0)	4.0718 (0,1.0)	3.6347 (0,1.0)	4.1937 (0,1.0)
$(60/-60)_5$	0.54258 (0,0.8)	0.48034 (0,0.3)	1.0376 (0,1.0)	3.5562 (0,1.0)	2.7342 (0,1.0)	3.4905 (0,1.0)
(75/-75)	0.21150 (0,0.8)	0.29005 (0.2,1.0)	0.76762 (0,1.0)	2.3612 (0,1.0)	0.22477* (1.0,0.4)	2.3185 (0,1.0)
$(75/-75)_2$	0.20724 (1.0,0.2)	0.27916* (0.8,1.0)	0.72067 (1.0,0)	2.2341 (0,1.0)	2.0421 (0,1.0)	2.2172 (0,1.0)
$(75/-75)_5$	0.20210* (1.0,0.3)	0.29429 (0.8,1.0)	0.70297 (0,1.0)	2.1239* (0,1.0)	1.7190 (0,1.0)	2.0769* (0,1.0)
90	0.070590 (0.8,0.6)	0.29334 (0.8,1.0)	0.71544 (1.0,1.0)	2.0200 (0,1.0)	1.5519 (0,0)	2.1892 (0,1.0)

Table 12. Maximum dimensionless sagging moment $(-\bar{M}_y)$ x 10^2 values.

Lamination (Number of layer and degree)	**Boundary conditions**					
	Group-A		**Group-B**		**Group-C**	
	A1	**A2**	**B1**	**B2**	**C1**	**C2**
	CSCS	**CSSC**	**FCFC**	**FCCF**	**FSFS**	**FSSF**
0	-1.5698 (0.2,0.2)	-1.6765 (0.8,0.2)	-0.23415 (1.0,0.5)	-4.3048 (0,0.6)	-3.2191 (0,0.4)	-5.1370 (0,0.6)
(15/-15)	-1.5903 (0.1,0.2)	-1.8024 (01,0.2)	-0.21179 (0,0)	-1.9348 (1.0,1.0)	-9.7810 (0,0)	-9.3130 (0,0)
$(15/-15)_2$	-1.3248 (0.2,0.2)	-1.4029 (0.2,0.2)	-0.24956 (0,0.5)	-1.9691 (0,0.6)	-3.9841 (0,0)	-4.0573 (0,0)
$(15/-15)_5$	-1.2034 (0.2,0.2)	-1.2142 (0.2,0.2)	-2.7184 (0,0.5)	-2.0627 (0,0.6)	-1.8199 (0,0.6)	-2.7541 (0,0.6)
(30/-30)	-1.2259 (0.1,0.2)	-1.2512 (0.1,0.2)	-1.1145 (0,0)	-3.3351 (1.0,1.0)	-7.8134 (0,0)	-7.1273 (0,0)
$(30/-30)_2$	-0.97902 (0.2,0.2)	-0.97209 (0.2,0.2)	-0.36436 (0.1,0.5)	-1.3133 (0.1,1.0)	-2.1584 (0,0)	-1.6397 (0.1,1.0)
$(30/30)_5$	-0.82669 (0.2,0.2)	-0.81437 (0.2,0.2)	-0.41116 (0.1,0.5)	-0.93143 (0,0.6)	-1.1606 (0.7,0.3)	-1.3010 (0,0.6)
(45/-45)	-0.83181 (0.9,0.9)	-0.82638 (0.1,0.1)	-1.4395 (1.0,1.0)	-2.1117 (1.0,1.0)	-5.4060 (0,0)	-5.2148 (0,0)
$(45/-45)_2$	-0.57818 (0.2,0.2)	-0.59639 (0.2,0.2)	-0.41564 (0.9,0.5)	-1.1167 (0.1,1.0)	-0.87503 (0.1,1.0)	-1.1590 (0.1,1.0)

$(45/-45)_5$	-0.46541 (0.2,0.2)	-0.47981 (0.2,0.2)	-0.46149 (0.9,0.5)	-0.87146 (0.1,1.0)	-0.72245 (0.9,0.5)	-0.86133 (0.1,1.0)
(60/-60)	-0.39908 (0.8,0.9)	-0.40235 (0.8,0.8)	-0.26637 (0.6,0.6)	-0.61979 (0,0.9)	-2.0792 (0,0)	-2.4285 (0,0)
$(60/-60)_2$	-0.29879 (0.8,0.9)	-0.33266 (0.8,0.7)	-0.23950 (0.1,0.5)	-0.60991 (0,0.9)	-0.57528 (0,0.9)	-0.60692 (0.8,0.9)
$(60/-60)_5$	-0.24881 (0.8,0.9)	-0.29873 (0.8,0.2)	-0.25543 (0.1,0.5)	-0.52014 (0,0.9)	-0.41357 (0,0.9)	-0.45680 (0,0.9)
(75/-75)	-0.18309 (0.2,0.1)	-0.20871 (0.8,0.1)	-0.23611 (1.0,0.7)	-0.34366* (0,0.7)	-0.20417* (0,0.5)	-0.35193 (0,0.7)
$(75/-75)_2$	-0.13453 (0.2,0.1)	-0.18294 (0.8,0.5)	-0.18523* (0.2,0.5)	-0.36144 (0,0.9)	-0.31581 (0,0.9)	-0.30127 (0,0.5)
$(75/-75)_5$	-0.11658* (0.2,0.1)	-0.17921* (0.8,0.5)	-0.18625 (0.8,0.5)	-0.369011 (0,0.9)	-0.27751 (0.8,0.5)	-0.29719* (0,0.5)
90	-0.076989 (0.7,0.5)	-0.13775 (0.8,0.5)	-0.23974 (0,0.2)	-0.44965 (0,0.8)	-0.38152 (0,0.2)	-0.41962 (0,0.8)

Table 13. Maximum dimensionless anticlockwise twisting moments ($+\bar{\mathbf{M}}_{\mathbf{xy}}$) x 10^2 values.

Lamination (Number of layer and degree)	**Boundary conditions**					
	Group-A		**Group-B**		**Group-C**	
	A1	**A2**	**B1**	**B2**	**C1**	**C2**
	CSCS	**CSSC**	**FCFC**	**FCCF**	**FSFS**	**FSSF**
0	0.10582 (0.1,0)	0.10056 (0.1,0)	0.0096258 (1.0, 0.9)	0.32716 (0.1,1.0)	0.27666 (1.0,1.0)	0.84155 (1.0,1.0)
(15/-15)	0.19413* (0.4,0.4)	0.21638 (1.0,0.35)	0 (0.55,0.5)	0.95138 (0,1.0)	0.92033 (0.1,0)	0.99062 (0,1.0)
$(15/-15)_2$	0.21069 (0.9,1.0)	0.18394* (0.1,0)	0 (0.55,0.5)	0.77547 (0.1,1.0)	0.72074 (0.1,0)	0.90679 (1.0,1.0)
$(15/-15)_5$	0.26287 (0.9,1.0)	0.23529 (0.1,0)	0 (0.55,0.5)	0.63396* (0.1,1.0)	0.55957 (0.1,0)	1.2273 (1.0,1.0)
(30/-30)	0.37690 (0,0.7)	0.43642 (1.0,0.35)	0 (0.55,0.5)	1.8048 (0.1,1.0)	1.6400 (0.1,0)	1.7257 (0.1,1.0)
$(30/-30)_2$	0.40642 (0.1,0)	0.38941 (0.1,0)	0.038991* (0,0.8)	1.3799 (0.1,1.0)	1.2188 (0.1,0)	1.4406 (0.1,1.0)
$(30/30)_5$	0.50274 (0.1,0)	0.47814 (0.1,0)	0.099199 (0,0.8)	1.0580 (0.1,1.0)	0.93478 (0.1,0)	1.8918 (1.0,1.0)
(45/-45)	0.41123 (0.35,1.0)	0.45653 (1.0,0.35)	0.21820 (0,0.9)	1.8287 (0.1,1.0)	1.6033 (0.9,1.0)	1.7188 (0.1,1.0)
$(45/-45)_2$	0.46058 (0.1,0)	0.47518 (0.1,0)	0.33466 (0,0.85)	1.5958 (0.1,1.0)	0.93871 (0.1,0)	1.4429 (0.1,1.0)
$(45/-45)_5$	0.54262 (0.1,0)	0.55702 (0.1,0)	0.38656 (0.05,0.8)	1.3549 (0.1,1.0)	1.0246 (1.0,1.0)	1.8868 (1.0,1.0)
(60/-60)	0.36794 (0.9.1.0)	0.52163 (0.65,0)	0.54942 (0.5,0.35)	1.1081 (0.15,1.0)	1.3459 (0,0.9)	1.1353 (0.15,1.0)
$(60/-60)_2$	0.42915 (0.9,1.0)	0.44217 (0.1,0)	0.38697 (0,0.9)	1.3963 (0,0.9)	1.2048 (0,0.9)	1.3643 (0,0.9)
$(60/-60)_5$	0.46745 (0.9,1.0)	0.49968 (1.0,0.9)	0.42696 (0.05,0.9)	1.3987 (0,0.9)	1.0133 (0,0.9)	2.0808 (1.0,1.0)
(75/-75)	0.26494	0.30164	0.24616	0.75834	0.29934*	0.76283*

	(0.1,0)	(0.65,0)	(0.5,0.65)	(0,0.9)	(0.95,0.05)	(0,0.9)
$(75/-75)_2$	0.23872 (0.1,0)	0.24089 (0.1,0)	0.23960 (0.95,0.05)	0.99036 (0,0.9)	0.67979 (0,0.9)	0.98234 (0,0.9)
$(75/-75)_5$	0.24318 (0.1,0)	0.26830 (1.0,0.9)	0.27396 (0.75,0.05)	0.99201 (0,0.9)	0.83143 (0,0)	1.5169 (1.0,1.0)
90	0.082923 (0.1,0)	0.090868 (1.0,0.9)	0.091709 (0.25,0.9)	0.47083 (0,0.9)	0.67186 (0,0)	0.84901 (1.0,1.0)

Table 14. Maximum dimensionless clockwise twisting moments ($-\bar{\mathbf{M}}_{\mathbf{xy}}$) x 10^2 values.

Lamination (Number of layer and degree)	**Boundary conditions**					
	Group-A		**Group-B**		**Group-C**	
	A1	**A2**	**B1**	**B2**	**C1**	**C2**
	CSCS	**CSSC**	**FCFC**	**FCCF**	**FSFS**	**FSSF**
0	-0.10582 (0.9,0)	-0.13963 (1.0,0)	-0.0096257 (0,0.9)	-0.72574 (0,1.0)	-0.27668 (0,1.0)	-0.94988 (0,1.0)
(15/-15)	-0.30532 (0.95,0)	-0.87353 (1.0,0)	-0.29627 (0,1.0)	-3.7005 (0,1.0)	-2.5996 (1.0,0)	-3.9482 (0,1.0)
$(15/-15)_2$	-0.32968 (0.9,0)	-0.56270 (1.0,0)	-0.15654 (0,1.0)	-2.3443 (0,1.0)	-1.7627 (0,1.0)	-2.8636 (0,1.0)
$(15/-15)_5$	-0.31240 (0.1,1.0)	-0.44582* (1.0,0)	-0.070885* (0,1.0)	-1.4828* (0,1.0)	-1.1324 (0,1.0)	-2.0658* (0,1.0)
(30/-30)	-0.67981 (0,1.0)	-2.0641 (1.0,0)	-1.1621 (0,1.0)	-6.3420 (0,1.0)	-5.0638 (1.0,0)	-6.8623 (0,1.0)
$(30/-30)_2$	-0.61925 (0.1,1.0)	-1.1130 (1.0,0)	-0.64255 (0,1.0)	-4.2020 (0,1.0)	-3.6183 (0,1.0)	-5.0799 (0,1.0)
$(30/30)_5$	-0.58977 (0.1,1.0)	-0.84858 (1.0,0)	-0.33025 (1.0,0)	-2.7530 (0,1.0)	-2.5109 (1.0,0)	-3.6750 (0,1.0)
(45/-45)	-0.66262 (0,1.0)	-2.6516 (1.0,0)	-2.3483 (1.0,0)	-7.8094 (0,1.0)	-7.3803 (0,1.0)	-8.8216 (0,1.0)
$(45/-45)_2$	-0.64120 (0.1,1.0)	-1.3953 (1.0,0)	-1.3268 (1.0,0)	-6.1542 (0,1.0)	-5.1283 (0,1.0)	-6.7371 (0,1.0)
$(45/-45)_5$	-0.61537 (0.1,1.0)	-1.0638 (1.0,0)	-0.73567 (0,1.0)	-4.8082 (0,1.0)	-3.5295 (0,1.0)	-4.9959 (0,1.0)
(60/-60)	-0.60564 (0.1,1.0)	-2.2147 (1.0,0)	-1.4400 (0,1.0)	-6.7441 (0,1.0)	-6.9561 (0,1.0)	-7.4234 (0,1.0)
$(60/-60)_2$	-0.53503 (0.1,1.0)	-1.2565 (1.0,0)	-0.85778 (0,1.0)	-5.7756 (0,1.0)	-4.5672 (0,1.0)	-6.1429 (0,1.0)
$(60/-60)_5$	-0.50874 (0.1,1.0)	-0.98648 (1.0,0)	-0.51668 (0.25,0.1)	-4.8823 (0,1.0)	-3.0881 (0,1.0)	-4.9211 (0,1.0)
(75/-75)	-0.38012 (0.1,1.0)	-0.94232 (1.0,0)	-0.24554 (0.75,0.9)	-3.7715 (0,1.0)	-0.29929* (0.05,0.1)	-4.4635 (0,1.0)
$(75/-75)_2$	-0.28331 (0.1,1.0)	-0.64519 (1.0,0)	-0.30212 (0.75,0.9)	-3.3922 (0,1.0)	-2.3282 (0,1.0)	-3.8133 (0,1.0)
$(75/-75)_5$	-0.26007* (0.1,1.0)	-0.53436 (1.0,0)	-0.30179 (0.25,0.1)	-2.9998 (0,1.0)	-1.6762 (0,1.0)	-3.1807 (0,1.0)
90	-0.082922 (0.1,1.0)	-0.15889 (1.0,0)	-0.091721 (0.25,0.1)	-1.2987 (0,1.0)	-0.67172 (0,1.0)	-1.4442 (0,1.0)

Table 15. Positive values of shell actions arranged in ascending order with respective shell options.

Shell action in dimensionless form	Dimensionless values (magnitude)	Dimensionless co-ordinates $(\bar{x}, \bar{y})$.	Shell actions
$\bar{N}_x$	0.040325	(0.0, 0.9)	FCFC (15/-15)
	0.40100	(0.0, 1.0)	FSFS $(15/-15)_5$
	0.46973	(0.0, 0.2)	CSCS $(45/-45)_5$
	0.48116	(0.0, 0.2)	CSSC $(45/-45)_5$
	0.51528	(0.1, 0.0)	FSSF $(45/-45)_5$
	1.9567	(0.2, 1.0)	FCCF $(15/-15)_5$
$\bar{N}_y$	0.030306	(0.0, 0.0)	CSCS $(60/-60)_5$
	0.022808	(1.0, 0.1)	CSSC $(60/-60)_5$
	0.078831	(0.4, 0.5)	FCFC $(75/-75)_5$
	3.3922	(0.1, 1.0)	FCCF $(75/-75)_5$
	3.4048	(0.9, 1.0)	FSFS $(75/-75)_5$
	4.3662	(0.1, 1.0)	FSSF $(60/-60)_5$
$\bar{N}_{xy}$	061852	(0.0, 1.0)	FCFC $(15/-15)_5$
	1.3023	(0.6, 0.4)	CSCS $(75/-75)_2$
	1.6731	(1.0, 0.0)	CSSC $(75/-75)_5$
	1.7139	(1.0, 0.1)	FSFS (75/-75)
	16.403	(0.0, 1.0)	FSSF $(15/-15)_5$
	16.507	(0.0, 1.0)	FCCF $(75/-75)_5$
$\bar{M}_x$	0.039772	(0.0, 1.0)	FCFC $(15/-15)_2$
	0.17327	(0.0, 1.0)	FSFS $(15/-15)_5$
	0.21481	(1.0, 0.0)	CSSC (15/-15)
	0.39304	(0.0, 0.8)	CSCS $(15/-15)_5$
	1.6426	(0.0, 1.0)	FCCF $(15/-15)_5$
	1.9954	(0.0, 1.0)	FSSF $(15/-15)_5$
$\bar{M}_y$	0.20210	(1.0, 0.3)	CSCS $(75/-75)_5$
	0.22477	(1.0, 0.4)	FSFS (75/-75)
	0.27916	(0.8, 1.0)	CSSC $(75/-75)_2$
	0.49085	(0.0, 1.0)	FCFC $(15/-15)_2$
	2.0769	(0.0, 0.0)	FSSF $(75/-75)_5$
	2.1239	(0.0, 1.0)	FCCF $(75/-75)_5$
$\bar{M}_{xy}$	0.038991	(0.0, 0.8)	FCFC $(30/-30)_2$
	0.18394	(0.1, 0.0)	CSSC $(15/-15)_2$
	0.19413	(0.4, 0.4)	CSCS (15/-15)
	0.29934	(0.95, 0.95)	FSFS (75/-75)
	0.63396	(0.1, 1.0)	FCCF $(15/-15)_5$
	0.76283	(0.0, 0.9)	FSSF (75/-75)

Table 16. Negative values of shell actions arranged in ascending order with respective shell options.

Shell action in dimensionless form	**Dimensionless values (magnitude)**	**Dimensionless co-ordinates $(\bar{x}, \bar{y})$**	**Shell actions**
	0.90650	(0.0, 0.5)	FCFC $(15/-15)_5$
	1.7173	(0.5, 0.4)	CSCS $(45/-45)_5$
	1.7772	(0.7, 0.3)	CSSC $(30/-30)_5$

$\overline{w}$	6.9547	(0.3, 0.5)	FSFS $(30/-30)_5$
	8.9958	(0.0, 0.5)	FCCF $(45/-45)_5$
	10.700	(0.7, 1.0)	FSSF $(30/-30)_5$
$\overline{N}_x$	0.34633	(0.0, 0.0)	FCFC (15/-15)
	0.65723	(0.5, 0.35)	CSSC (15/-15)
	0.91057	(0.5, 0.35)	CSCS (15/-15)
	3.3393	(0.0, 0.0)	FSFS $(15/-15)_5$
	8.5746	(0.0, 1.0)	FCCF $(15/-15)_5$
	9.7474	(0.0, 1.0)	FSSF $(15/-15)_5$
$\overline{N}_y$	1.2435	(0.5, 0.65)	CSCS $(75/-75)_5$
	1.2501	(0.5, 0.65)	CSSC (75/-75)
	2.0035	(0.0, 1.0)	FCCF (75/-75)
	2.4180	(1.0, 1.0)	FCFC $(75/-75)_5$
	9.2261	(0.0, 0.0)	FSFS (75/-75)
	25.284	(0.0, 1.0)	FSSF $(75/-75)_5$
$\overline{N}_{xy}$	0.62341	(0.0, 0.0)	FCFC $(15/-15)_5$
	1.3481	(0.6, 0.6)	CSCS $(75/-75)_5$
	1.3545	(0.4, 0.4)	CSSC $(75/-75)_5$
	3.0514	(0.0, 0.9)	FCCF $(75/-75)_5$
	12.101	(0.0, 0.0)	FSFS $(15/-15)_5$
	12.705	(0.0, 0.0)	FSSF $(15/-15)_5$
$\overline{M}_x$	0.02100	(0.7, 0.7)	FCFC $(15/-15)_2$
	0.17348	(0.7, 0.2)	CSSC $(15/-15)_5$
	0.17505	(0.3, 0.8)	CSCS $(15/-15)_5$
	0.29656	(0.3, 0.8)	FSFS $(15/-15)_5$
	0.45327	(0.1, 0.1)	FCCF $(30/-30)_5$
	0.50554	(0.2, 1.0)	FSSF $(15/-15)_5$
$\overline{M}_y$	0.11658	(0.2, 0.1)	CSCS $(75/-75)_5$
	0.17921	(0.8, 0.5)	CSSC $(75/-75)_5$
	0.18523	(0.2, 0.5)	FCFC $(75/-75)_2$
	0.20417	(0.0, 0.5)	FSFS (75/-75)
	0.29719	(0.0, 0.5)	FSSF $(75/-75)_5$
	0.34366	(0.0, 0.7)	FCCF (75/-75)
$\overline{M}_{xy}$	0.070885	(0.0, 1.0)	FCFC $(15/-15)_5$
	0.26007	(0.1, 1.0)	CSCS $(75/-75)_5$
	0.29929	(0.05, 0.1)	FSFS (75/-75)
	0.44582	(1.0, 0.0)	CSSC $(15/-15)_5$
	1.4828	(0.0, 1.0)	FCCF $(15/-15)_5$
	2.0658	(0.0, 1.0)	FSSF $(15/-15)_5$

Table 17. Relative performance matrix

	Ten-layer laminated Shell	
Positive	**CSCS**	**FCFC**
$\overline{N}_x$	1	0
$\overline{N}_y$	1	0
$\overline{N}_{xy}$	0	1

$\bar{M}_x$	1	0
$\bar{M}_y$	1	0
$\bar{M}_{xy}$	0	0
Negative	**CSCS**	**FCFC**
$\bar{w}$	0	1
$\bar{N}_x$	0	0
$\bar{N}_y$	1	0
$\bar{N}_{xy}$	0	1
$\bar{M}_x$	1	0
$\bar{M}_y$	1	0
$\bar{M}_{xy}$	0	1
Total	7	4

REFERENCES

[1] P. C. Kohnke and W. C. Schnobrich, "Analysis of eccentrically stiffened cylindrical shells," *Journal of the Structural Division*, vol. 98, no. 7, pp. 1493-1510, 1972, doi: 10.1061/JSDEAG.000327.

[2] S. Sahoo and D. Chakravorty, "Bending of composite stiffened hypar shell roofs under point load," *Journal of Engineering Mechanics*, vol. 134, no. 6, pp. 441-454, 2008, doi:10.1061/(ASCE)0733-9399(2008)134:6(441).

[3] A. K. Miri and A. Nosier, "Interlaminar stresses in antisymmetric angle-ply cylindrical shell panels," *Composite Structures*, vol. 93, no. 2, pp. 419-429, 2011, doi:10.1016/j.compstruct.2010.08.038.

[4] P. B. Chowdhury, A. Mitra and S. Sahoo, "Relative performance of antisymmetric angle-ply laminated stiffened hypar shell roofs with cutout in terms of static behavior," *Curved and Layered Structures*, vol. 3, no. 1, pp. 22-46, 2016, doi:10.1515/cls-2016-0003.

[5] P. Kumari and S. Kar, "Static behavior of arbitrarily supported composite laminated cylindrical shell panels: an analytical 3D elasticity approach," *Composite Structures*, vol. 207, pp. 949-965, 2019, doi:10.1016/j.compstruct.2018.09.035.

[6] C. Zhu, B. Shi, C. Zhou and J. Yang, "Vibration analysis of laminated composite cylindrical shells with various fibre orientations," *EASD Procedia Eurodyn*, pp. 551-561, 2020, doi:10.47964/1120.9043.19371.

[7] F. Savine, F. X. Irisarri, C. Julien, A. Vincenti and Y. Guerin, "A component-based method for the optimization of stiffener layout on large cylindrical rib-stiffened shell structures," *Structural and Multidisciplinary Optimization*, vol. 64, no. 4, pp. 1843-1861, 2021, doi:10.1007/s00158-021-02945-9.

[8] A. M. Najafov, A. H. Sofiyev, D. Hui, F. Kadioglu, N. V. Dorofeyskaya and H. Huang, "Non-linear dynamic analysis of symmetric and antisymmetric cross-ply laminated orthotropic thin shells," *Meccanica,* vol. 49, pp. 413-427, 2014, doi:10.1007/s11012-013-9802-z.

[9] A. Kumar, A. Chakrabarti and P. Bhargava, "Vibration analysis of laminated composite skew cylindrical shells using higher order shear deformation theory," *Journal of Vibration and Control*, vol. 21, no. 4, pp. 725-735, 2015, doi:10.1177/1077546313492555 .

[10] K. K. Viswanathan and S. Javed, "Free vibration of anti-symmetric angle-ply cylindrical shell walls using first-order shear deformation theory," *Journal of Vibration and Control*, vol. 22, no. 7, pp. 1757-1768, 2016, doi:10.1177/1077546314544893.

[11] B. Tong, Y. Li, X. Zhu and Y. Zhang, "Three-dimensional vibration analysis of arbitrary angle-ply laminated cylindrical shells using differential quadrature method," *Applied Acoustics*, vol. 146, pp. 390-397, 2019, doi: 10.1016/j.apacoust.2018.11.031.

[12] S. Mohammadrezazadeh and A. A. Jafari, "Nonlinear vibration analysis of laminated composite angle-ply cylindrical and conical shells," *Composite Structures*, vol. 255, article id. 112867, 2021, doi:10.1016/j.compstruct.2020.112867.

[13] B. Y. Zhang and W. Zhang, "Theory of nonlinear vibrations for antisymmetric cross-ply bi-stable laminated shells," *Shock and Vibration*, vol. 2021, no. 1, article id. 3303512, 2021, doi:10.1155/2021/3303512.

[14] P. B. Chaudhuri, A. Mitra and S. Sahoo, "A parametric study of higher-mode natural frequencies of composite stiffened cylindrical shell with cut-out," *Engineering Transactions*, vol. 71, no. 1, pp. 81-109, 2023, doi: 10.24423/EngTrans.2456.20230126.

[15] V. Keshav, S. N. Patel and R. Kumar, "Non-linear stability and failure of laminated composite stiffened cylindrical panels subjected to in-plane impulse loading," *Structure*, vol. 29, pp. 360-372, 2021, doi:10.1016/j.istruc.2020.11.021.

[16] S. Sahoo, "Buckling behavior of laminated composite stiffened cylindrical shell panels having cutout for different parametric variations," *Proc. IMechE Part C: Journal of Mechanical Engineering Science*, vol. 236, no. 22, pp. 10987-11007, 2022 doi:10.1177/09544062221100613.

[17] K. Liang and Z. Li, "A novel nonlinear FE perturbation method and its application to stacking sequence optimization for snap-through response of cylindrical shell panel," *Computers & Mathematics with Applications*, vol. 112, pp. 154-166, 2022, doi:10.1016/j.camwa.2022.03.002.

[18] M. Sun, H. Zhou, C. Liao, Z. Zhang, G. Zhang, S. Jiang and F. Zhang, "Stable characteristics optimization of anti-symmetric cylindrical Shell with laminated carbon fiber composite," *Materials*, vol. 15, no. 3, article id. 933, 2022, doi: 10.3390/ma15030933.

[19] Z. Dai and Y. Kiani, "Stability of higher-order lattice composite cylindrical shell reinforced with graphene platelets by means of a Chebyshev collocation-based semi-analytical approach," *Engineering Structures*, vol. 296, article id. 116952, 2023, doi:10.1016/j.engstruct.2023.116952.

[20] L. Zhang, L. Zhao, L. Pan and J. Gao, "Research progress of composite cylindrical shells," *Polymer Composites,* vol. 44, no. 11, 7298-7316, 2003, doi:10.1002/pc.27659.

[21] S. Sahoo and D. Chakravorty, "Deflections, forces, and moments of composite stiffened hypar shell roofs under concentrated load," *The Journal of Strain Analysis for Engineering Design*, vol. 41, no. 1, pp. 81-97, 2006, doi:10.1243/030932405X309.

[22] S. Y. P. Chang, "Analysis of eccentrically stiffened plates," University of Missouri-Columbia, 1973, 7418494.

[23] M. P. Rossow and A. K. Ibrahimkhail, "Constraint method analysis of stiffened plates" *Computers & Structures*, vol. 8, no. 1, pp. 51-60, 1978, doi:10.1016/0045 7949(78)90159-1.

[24] G. Sinha, A. H. Sheikh and M. Mukhopadhyay, "A new finite element model for the analysis of arbitrary stiffened shells," *Finite Elements in Analysis and Design,* vol. 12, no. 3-4, pp. 241-271, 1992, doi:10.1016/0168-874X(92)90036-C.

[25] S. Sahoo, "Laminated composite stiffened cylindrical shell panels with cutouts under free vibration," *International Journal of Manufacturing, Materials, and Mechanical Engineering*, vol. 5, no. 3, pp. 37-63, 2015, doi: 10.4018/IJMMME.2015070103 .